Oecologia (2011) 165:289–299
DOI 10.1007/s00442-010-1800-4

PHYSIOLOGICAL ECOLOGY - ORIGINAL PAPER

Predicting tropical plant physiology from leaf and canopy spectroscopy

Christopher E. Doughty · Gregory P. Asner · Roberta E. Martin

Received: 11 November 2009 / Accepted: 14 September 2010 / Published online: 21 October 2010

Abstract A broad regional understanding of tropical forest leaf photosynthesis has long been a goal for tropical forest ecologists, but it has remained elusive due to difficult canopy access and high species diversity. Here we develop an empirical model to predict sunlit, light-saturated, tropical leaf photosynthesis using leaf and simulated canopy spectra. To develop this model, we used partial least squares (PLS) analysis on three tropical forest datasets (159 species), two in Hawaii and one at the biosphere 2 laboratory (B2L). For each species, we measured light-saturated photosynthesis (A), light and CO_2 saturated photosynthesis (A_{max}), respiration (R), leaf transmittance and reflectance spectra (400–2,500 nm), leaf nitrogen, chlorophyll a and b, carotenoids, and leaf mass per area (LMA). The model best predicted A [$r^2 = 0.74$, root mean square error (RMSE) = 2.9 μmol m^{-2} s^{-1})] followed by R ($r^2 = 0.48$), and A_{max} ($r^2 = 0.47$). We combined leaf reflectance and transmittance with a canopy radiative transfer model to simulate top-of-canopy reflectance and found that canopy spectra are a better predictor of A (RMSE = 2.5 ± 0.07 μmol m^{-2} s^{-1}) than are leaf spectra. The results indicate the potential for this technique to be used with high-fidelity imaging spectrometers to remotely sense tropical forest canopy photosynthesis.

Communicated by Gerardo Avalos.

Electronic supplementary material The online version of this article (doi:10.1007/s00442-010-1800-4) contains supplementary material, which is available to authorized users.

C. E. Doughty (✉) · G. P. Asner · R. E. Martin
Department of Global Ecology,
Carnegie Institution, Stanford, CA 94305, USA
e-mail: chris.doughty@ouce.ox.ac.uk

Keywords Photosynthesis · Tropical forests · Spectranomics · Spectra · Gas exchange · Remote sensing · CAO

Introduction

Tropical forest net primary production plays an important role in the global carbon cycle (Field et al. 1998), but there is much debate on whether tropical forests are net sources or sinks of CO_2 to the atmosphere (Grace et al. 1995; Phillips et al. 1998; Saleska et al. 2003). It has been clear for some time that a better understanding of tropical forest physiology and leaf-level gas exchange could shed light on these questions, but the difficulty of accessing tropical forest canopies, along with their high species diversity, has so far hindered the development of a broad regional understanding.

High-resolution remote sensing may be an ideal technique for acquiring data that would improve our understanding of tropical forest physiology over large geographic areas. However, remote sensing of physiology has been attempted at the leaf and canopy scales with mixed results. Sims and Gamon (2002) detected photosynthetic stress at the leaf level in multiple species via xanthophyll pigment changes with the photochemical reflectance index (PRI) (Sims and Gamon 2002). Asner et al. (2004) measured drought stress in an Amazon tropical forest by space-borne imaging spectroscopy of the canopy water content. These studies showed the potential of the systems to remotely detect physiology, but the sensors used were not designed to identify physiological differences between individual species.

To understand the physiology of tropical forests, we first must understand leaf chemistry. Although there may be

broad shifts in leaf chemistry with soil fertility, these tend to be modest in size and indeed perhaps smaller than the range of variation seen among co-occurring species in terms of their leaf chemistry. For example, the dominant landscape-level influence over foliar nitrogen (N) and phosphorus (P) ratios in the humid tropics is species variability, not substrate (Townsend et al. 2007). Several physiologically important chemicals, such as N, are directly expressed in the leaf spectra. Studies have shown that foliar concentrations of N, chlorophyll (Chl) *a* and *b*, carotenoids, water, and leaf mass per area (LMA) can be predicted using the reflectance and transmittance of light from individual leaves and canopies (Curran 1989; Sims and Gamon 2002; Smith et al. 2003a, b). Laboratory and modeling studies have also demonstrated how these chemicals influence leaf spectral properties (Feret et al. 2008; Jacquemoud and Baret 1990).

Relationships between leaf spectral and chemical properties have been developed using partial least squares (PLS) regression analysis. This technique does not focus on individual bands but uses the entire leaf spectral continuum. Previous studies using this technique showed that LMA, Chl *a* and *b*, and N concentrations are highly correlated with the reflectance and transmittance spectra of tropical species (Asner et al. 2009). Moreover, each spectral band is weighted to determine its relative importance in predicting chemical constituents, and these band weights indicate the spectral features (involving contiguous wavelength regions) that are most important to predict a variable (Haaland and Thomas 1988). For example, Asner et al. (2009) found that PLS weightings for LMA were strong throughout the 750- to 2,500-nm range because this region is dominated by variations in leaf water content and leaf thickness (Asner et al. 2009), both of which are related to LMA (Jacquemoud and Baret 1990). N weightings were associated with wavelengths absorbed by Chl *a* and *b* in the visible (400–700 nm), the spectral red edge (700–760 nm), and proteins in the shortwave infrared range (1,300–2,500 nm) (Gitelson and Merzlyak 1997; Kokaly 2001; Smith et al. 2003a).

Leaf photosynthesis is generally correlated with leaf chemistry. A worldwide foliar dataset indicates that 82% of all variation in photosynthetic capacity (by mass) can be explained by LMA and N (on a log–log scale) (Wright et al. 2004). A similar study used 53 tropical species and found that LMA predicted mass-based rates of assimilation and respiration and that leaf life span predicted many other traits (Poorter and Bongers 2006). Despite these advances, few studies have considered the three-way connection between the spectroscopic, chemical, and physiological properties of foliage, although many have considered various aspects of two out of three of these areas, particularly as to how spectral band ratios [e.g., normalized difference vegetation index (NDVI)] scale with leaf and canopy chemistry and physiology (e.g., Sellers 1985; Verma 1993). However, the full spectroscopic signatures of species have not been considered in this context.

We combined leaf physiological, chemical, and spectral data from 159 tropical species gathered on three field campaigns, two in Hawaii and one at the biosphere 2 laboratory (B2L) in Arizona. We tested our ability to predict leaf physiological properties from leaf spectra using empirically based models. We then used observed relationships between leaf chemical/spectral and chemical/physiological properties to understand the relationships between the spectral/physiological properties. Finally, we scaled the leaf spectra to the canopy level using a radiative transfer model (Asner and Martin 2008) and developed models predicting physiological properties using simulated canopy spectra. We addressed the following questions: Can tropical leaf photosynthetic capacity and other physiological properties be predicted from full spectral range (400–2,500 nm) leaf spectroscopy? What is the relationship among spectral, chemical, and physiological properties, in the context of spectroscopic remote sensing? Are canopy spectra more or less useful than leaf spectra for the prediction of photosynthetic capacity and other physiological properties?

Methods

Study sites

We collected foliar material and measured the physiological properties of 149 species in two tropical forest sites on Hawaii island in January and April of 2009 and ten species in the tropical rainforest biome and the display center of B2L (Dempster 1999) in October 2004. We emphasized collecting data from many species versus repeating measurements on individual species because much of the variability in leaf nutrient concentrations can be explained by species variability (Townsend et al. 2007). These species represent a wide variety of regeneration strategies. In the first Hawaii campaign, we chose a site near to the Institute for Pacific Islands Forestry in Hilo, Hawaii, located on the windward, wet side of the island (approx. 3,500 mm year^{-1}). This site consists of young basalt substrate (approx. 220 years old) with Hawaiian endemic and common exotic species. We measured sunlit intact leaves from 11 species. For the second collection, we measured 138 tropical tree and palm species at sites spread across the windward side of the island (mean annual precipitation 2,000–4,000 mm). These samples were taken mainly from non-native, full-grown trees grown in botanical gardens near Hilo. At B2L, we measured ten canopy rainforest tree species, sampling ten leaves still connected

to the tree. The tropical rainforest biome in B2L has a temperature (approx. 25°C) and humidity (approx. 65%) typical of a Neotropical forest. The tropical forest section of the display center was kept under similar conditions to accommodate the variety of tropical rainforest species growing there.

Leaf spectra

We measured full-range (400–2,500 nm) hemispherical reflectance and transmittance spectra of six leaves of each of the 149 species tested using a custom-designed spectrometer with 2.7-nm sampling and 1.0-nm reporting (FR-Pro with Select Test detectors and a custom exit slit to maximize signal-to-noise performance; Analytical Spectra Devices, Boulder, CO), an integrating sphere modified for high-resolution spectroscopic analysis with interior sphere walls refitted with Spectralon coating (Labsphere, Durham, NH), and a custom-built 2-Solar illumination collimator (Carnegie Institution, Stanford, CA) (http://spectranomics.stanford.edu/technical_information). Measurements were collected with a 136-ms integration time per spectrum. The spectra were then calibrated for dark current and stray light and referenced to a calibration block (Spectralon) within the integrating sphere. We measured reflectance and transmittance immediately after separating the leaf from each branch.

Leaf chemistry

The leaves remaining on the branches were used for chemical analysis. We measured the wet weight of ten individual leaves of each of the 149 species using a balance and the area of these leaves using a leaf area meter (Li-Cor Biosciences, Lincoln, NE). Prior to measurement, the leaves were stored on ice in coolers for usually less than 3 h. The samples were then dried at 65°C for >72 h and re-weighed for dry mass. Dried samples were sent to the Carnegie Institution where leaves were ground in a 20-mesh Wiley mill, and total N concentrations were determined using combustion–reduction analysis (Costech, Ventura, CA). In the field, 30 disks (area 0.8 cm^2) were punched out of each of ten randomly selected leaves ($n = 300$ per species) of each of the 149 species and then frozen with liquid N. The samples were transferred to a −80°C freezer, where they were held until later analysis for Chl *a* and *b* and carotenoid concentrations (Asner et al. 2009). the frozen leaf disks were ground in a chilled mortar with 100% acetone, a small amount of quartz sand, and $MgCO_3$ to prevent acidification. Following centrifugation for 3 min at 3,000 rpm, the absorbance of the supernatant was measured using a dual-beam scanning UV–Vis spectrophotometer (Lambda 25; Perkin Elmer, Beaconsfield, UK). Chl *a* and *b* and carotenoid concentrations were determined using multi-wavelength analysis at 470, 645, 662, and 710 nm (Lichtenthaler 2001).

Leaf physiology

We used a portable gas exchange system (model LI 6400; Li-Cor Biosciences) to measure leaf photosynthesis and respiration. In Hawaii, we measured gas exchange three to four times on each of two leaves of 149 species for A [1,000 µmol m^{-2} s^{-1} photosynthetic photon flux density (PPFD), 400 ppm CO_2, 25°C], A_{max} (1,000 µmol m^{-2} s^{-1} PPFD, 1,500 ppm CO_2, 25°C), and R (0 µmol m^{-2} s^{-1} PPFD, 400 ppm CO_2, 25°C). We relied on cut branches for most species. We first cut a large branch (>1 m) with sunlit leaves off the tree. We then cut off a smaller branch from this larger branch while the stem was submerged in water to restore hydraulic conductivity before we made the physiology measurements. At B2L, we measured A (1,500 µmol m^{-2} s^{-1} PPFD, 400 ppm CO_2, 25°C) on ten leaves on each of ten species on live branches. To screen for erroneous data, we removed very low measurements ($A < 4$ µmol m^{-2} s^{-1}) and unstable measurements (if the standard deviation of our three measurements was >15% of the mean). Unstable measurements indicated a stress response of the plant to being cut and that the photosynthetic data were likely unreliable. Using these thresholds, we removed 27% of small tree species, 38% of medium tree species, 19% of large tree species, 68% of palm species, 29% of vine species, and 25% of shrub species [Electronic Supplementary Material (ESM) Table 1].

On a subset of these species ($n = 11$ in Hawaii and $n = 10$ at B2L), we measured V_{cmax} and J_{max}. We calculated V_{cmax} (the maximum velocity of Rubisco for carboxylation) and J_{max} (the maximum rate of electron transport) using a non-linear curve fitting program (Farquhar et al. 1980; Sharkey et al. 2007). For A_{ci} curves, we varied CO_2 concentrations (from 400, 300, 200, 100, 50, 0, 400, 700, 900, 1,200 ppm) while keeping other environmental conditions stable (in Hawaii: 1,000 µmol m^{-2} s^{-1} PPFD, 25°C leaf temperature; in B2L: 1,500 µmol m^{-2} s^{-1} PPFD, 30°C leaf temperature). For light curves, we varied PPFD (from 1,000, 2,000, 500, 250, 100, 50, 0 µmol m^{-2} s^{-1}) while keeping other environmental conditions stable (in Hawaii: 370 ppm CO_2, 25°C; in B2L: 400 ppm CO_2, 30°C) on two to five leaves per species. We tested the following species for V_{cmax} and J_{max}: in Hawaii, *Psidium cattleianum*, *Metrosideros polymorpha*, *Melochia umbellate*, *Melastoma septemnervium*, *Macaranga taitensis*, *Buddleja davidii*, *Trema orientalis*, *Spathodea campanulata*, *Pluchea carolinensis*, *Falcatoria mollucana*; in B2L, *Clitoria racemosa*, *Pachira aquatica*, *Persea americana*, *Bixa orellana*, *Cecropia obtusifolia*, *Cananga odorata*, *Ceiba pentandra*, *Ficus nitida*, *Inga sapinoides*, and *Trichilia alba*. Most physiological

measurements were collected between 7 a.m. and 12 p.m. local time (between 8 and 10 a.m. in B2L) to ensure that photosynthesis was not limited by hot midday conditions.

Spectral–chemical–physiological analysis

Principal components analysis (PCA) (Matlab; MathWorks, Natick, MA) was used to compare leaf physiological and chemical properties following Wright et al. (2004). This technique takes a group of variables (in our case, A, N, leaf pigments, and LMA) and calculates several principal components. The first PC is a vector through multi-dimensional trait–space that best explains the main linear trend through the data. The data in these analyses are then $\log_{10}$ transformed because they are right skewed.

We also used PLS regression analysis to link leaf hemispherical reflectance and transmittance spectra to A, A_{max}, R, V_{cmax}, J_{max}, LMA, N, and Chl a and b. To avoid overfitting the number of factors used in the analysis, we minimized the mean square error through a process of cross validation for each model. This process iteratively generates regression models while removing one sample from the input data set until the mean square error is minimized. We calculated spectral weightings generated during the PLS analysis by taking the weightings for the top two latent vectors, multiplying these by the percentage variance they explained, and then adding them together. Leaf transmittance was more strongly correlated with physiological and chemical properties than were reflectance or absorbance, so unless otherwise specified, we report here leaf transmittance for the PLS regressions. We define our regressions as strongly correlated ($r^2 > 0.7$), moderately correlated ($0.7 < r^2 > 0.5$), or weakly correlated ($r^2 < 0.5$).

Canopy modeling

To test whether the leaf-level PLS regression analysis would apply at the canopy scale, we generated canopy reflectance measurements using a radiative transfer model described in Asner and Martin (2008). This model simulates top-of-canopy spectral reflectance using measured leaf-level hemispherical reflectance and transmittance for each species, leaf area index (LAI), canopy leaf angle distribution (LAD), other canopy architectural parameters, and geometry, which includes solar zenith and azimuth angle and sensor viewing zenith and azimuth angles.

We initially used a fixed set of parameters to simulate canopy spectra, namely, LAI = 5, LAD = uniform and constant viewing and solar geometry (nadir viewing and 30° solar zenith angle). Each simulated canopy spectrum comprised 220 bands with a 10-nm bandwidth covering the 400 to 2,500-nm wavelength region, similar to the spectral data provided by the Airborne Visible and Infrared Imaging Spectrometer (AVIRIS; Green et al. 1998). We also created ten additional canopy spectra per species with varying LAI and LAD. For each species, we averaged three simulations together, each with a randomly generated LAI of between 3 and 7, and a randomly generated LAD (any of five: plagiophile, planophile, erectophile, uniform, spherical; Myneni et al. 1989). This allowed us to evaluate the effects of varying canopy-level LAI and LAD properties on this technique since any airborne campaign will fly over forests with unknown LAI and LAD.

Determining which spectral features to use

We tested which spectral features minimize the root mean square error (RMSE) of the PLS regressions at the canopy scale. Variable LAI or LAD in the canopy simulations increase spectral variability in the near-infrared (NIR) spectrum. This spectral variability reduced the strength of the PLS regressions. However, there is spectral information useful for predicting leaf chemical properties in the NIR (Feret et al. 2008; Jacquemoud and Baret 1990), such as for predicting LMA (Asner and Martin 2008). To determine whether including this spectral information improves the canopy-level predictions more than it is decreased by the spectral variability from unknown LAI and LAD, we consecutively tested the PLS regressions at various wavelengths, starting at 400–600 nm and increasing the range being tested by 50-nm increments until we had analyzed the entire 400–2,500-nm spectrum. At each wavelength, we made PLS regressions on all ten canopy simulations with unknown LAI and LAD and recorded the RMSE.

Results

Leaf chemistry and spectra

Averaged leaf spectra collected in Hawaii were of a similar shape and magnitude to those from other tropical forests (Fig. 1) (Castro-Esau et al. 2006; Lee et al. 1990). However, there were significant differences in leaf reflectance and transmittance between B2L and Hawaii spectra ($P < 0.05$) at most wavelengths. Standard deviations (SD) of Hawaiian leaf transmittance peaked in the visible spectrum at approximately 550 nm (SD 0.05 vs. 0.035 for B2L) and peaked in the NIR spectrum between 720 and 1,830 nm (SD 0.075; B2L peaked at wavelengths >2,200 nm with a SD of 0.053).

Average Hawaiian leaf chemical values and LMA were within the range of other tropical forests (Table 1) (McGroddy et al. 2004; Townsend et al. 2007). Average leaf chemical values and LMA for B2L were significantly higher than the Hawaiian LMA ($P < 0.001$), N ($P < 0.001$), and Chl a ($P < 0.05$) and b ($P < 0.05$) in this study.

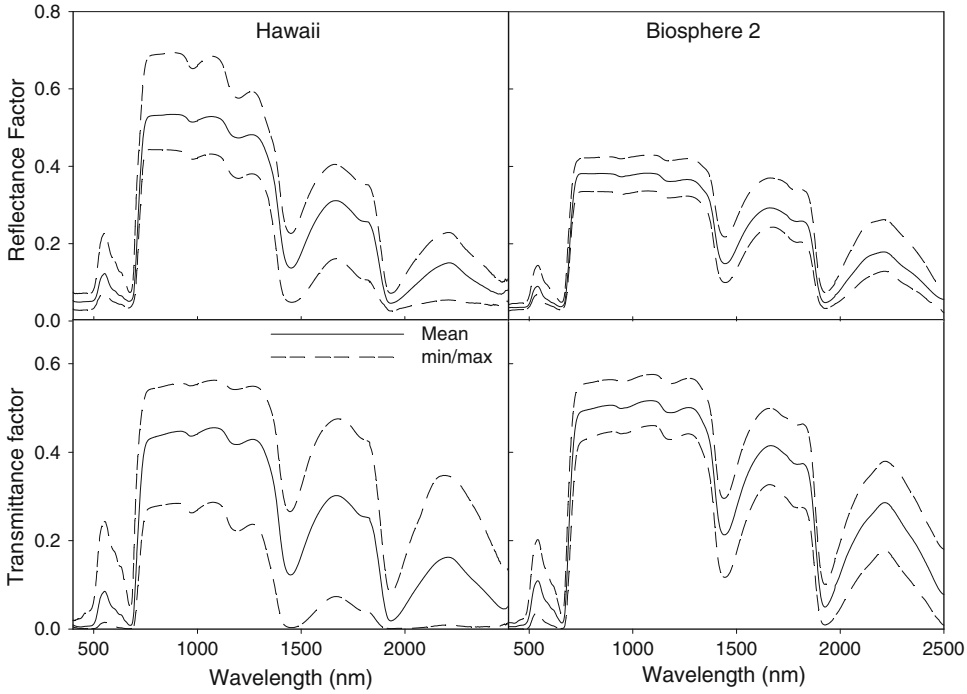

Fig. 1 Mean leaf reflectance (*top*) and transmittance (*bottom*) for species collected in Hawaii (*left*) ($n = 149$) and the B2L tropical rainforest modules (*right*) ($n = 10$)

Photosynthesis measurements

Average light-saturated photosynthesis at ambient CO_2 (A), light-saturated photosynthesis at high CO_2 (A_{max}), and respiration (R) from B2L and Hawaii were similar to those reported for other tropical forests (Table 1) (Domingues et al. 2007). Average A was significantly greater in B2L than in Hawaii ($P < 0.05$). We calculated V_{cmax}, and J_{max} on a subset of Hawaiian ($n = 11$) and B2L ($n = 10$) species and did not find significant differences for V_{cmax}, and J_{max} between the Hawaii and the B2L datasets ($P > 0.05$). These values were similar to those of other upper canopy tropical forest tree species (Domingues et al. 2007). Data from palms were thrown out at a significantly higher rate than those for other functional types because palms often had very low measured A, possibly indicating that the method is less effective on palms.

Leaf chemical and physiological properties

We investigated the correlation patterns among photosynthetic capacity, LMA, leaf N and pigment concentrations using PCA. The first PC along the axis of data between N, LMA, A_{mass}, Chl a, and Chl b explained 83% of the variation, with coefficients of N = −0.42, LMA = 0.32, A_{mass} = −0.52, Chl a = −0.47, and Chl b = −0.49. The first PC along the axis of the data between N, LMA, and A_{mass} explained 86% of the variation, with coefficients of N = −0.42, LMA = 0.54, and A_{mass} = −0.73. A three-way trait relationship between N, LMA, and A_{mass} is shown in Fig. 2. All data were $\log_{10}$ transformed because the data were right skewed.

PLS regressions

We first used PLS regression analysis on the B2L and the Hawaii datasets individually and then combined the datasets to examine how well leaf chemical properties could be predicted from leaf transmittance properties (Fig. 3). The B2L spectral dataset more accurately predicted leaf chemical properties than did the Hawaiian spectral dataset. Combining both datasets, there was a strong correlation ($r^2 = 0.74$, RMSE = 2.85 μmol m^{-2} s^{-1}) between A and leaf spectra ($n = 159$) (Fig. 3). Correlations were strong for LMA ($r^2 = 0.90$, RMSE = 18.7 g m^{-2}), N ($r^2 = 0.83$, RMSE = 0.45 g), and moderate for leaf pigments (Chl a, $r^2 = 0.66$; Chl b, $r^2 = 0.67$, carotenoid, $r^2 = 0.60$). R ($r^2 = 0.48$) and A_{max} ($r^2 = 0.47$) were weakly correlated. Predictions of V_{cmax} and J_{max} were tested on a subset of the photosynthesis data ($n = 40$ leaves, 11 species). There was a positive correlation with J_{max} ($r^2 = 0.52$, RMSE = 39 μmol m^{-2} s^{-1}) and a weaker correlation with V_{cmax} ($r^2 = 0.39$, RMSE = 36 μmol m^{-2} s^{-1}).

The spectral weightings used to predict photosynthesis were of similar shape to the spectral weightings of leaf pigments, LMA, and N, with large weightings in the visible region and smaller weightings in the NIR region (Fig. 4). To quantify this relationship, we regressed leaf pigments, LMA, and N weightings against weightings for A. N showed a strong correlation with A ($r^2 = 0.76$), but

Table 1 Chemical and physiological values, number of species sampled, and maximum, and minimum values from the B2L and two Hawaii field campaigns

Chemical and physiological values[a]	Date and site		
	2004, Biosphere	2009, Hawaii	2009, Hawaii IPIF
Chlorophyll *a* (%)	4.7 ± 2.5, *n* = 10	3.7 ± 2.5, *n* = 138	3.4 ± 1.3, *n* = 11
Max	15.7	14.4	5.8
Min	1.1	0.8	1.6
Chorophyll *b* (%)	1.8 ± 0.1, *n* = 10	1.40 ± 0.1, *n* = 138	1.2 ± 0.5, *n* = 11
Max	6.7	5.3	2.2
Min	0.4	0.3	0.5
LMA (g m^{-2})	83 ± 28, *n* = 10	118 ± 56, *n* = 138	106 ± 50, *n* = 11
Max	190	308	215
Min	38	22	64
Leaf nitrogen (%)	2.6 ± 0.6, *n* = 10	1.7 ± 0.8, *n* = 134	1.6 ± 0.6, *n* = 11
Max	3.8	5.3	2.7
Min	0.6	0.6	0.9
A (μmol m^{-2} s^{-1})	9.7 ± 4.8, *n* = 10	8.2 ± 2.9, *n* = 86	14.0 ± 6.4, *n* = 11
Max	21.2	14.8	31.5
Min	1.2	4.0	9.4
A_{max} (μmol m^{-2} s^{-1})	24.3 ± 4.0, *n* = 10	15 ± 5.4, *n* = 90	20.5 ± 5.9, *n* = 11
Max	33.3	29.9	34.1
Min	16.9	4.9	12.7
R (μmol m^{-2} s^{-1})	−1.4 ± 0.4, *n* = 10	−1.2 ± 0.6, *n* = 117	−1.1 ± 0.4, *n* = 11
Max	−1.0	0.2	−0.6
Min	−2.1	−2.5	−1.9
V_{cmax} (μmol m^{-2} s^{-1})	87.1 ± 22, *n* = 10		85 ± 36, *n* = 11
Max	128.3		203
Min	60		25.9
J_{max} (μmol m^{-2} s^{-1})	123.5 ± 25, *n* = 10		109 ± 40, *n* = 11
Max	170.5		287.2
Min	88.4		53.2

A Light-saturated photosynthesis, A_{max} light- and CO_2-saturated photosynthesis, *R* respiration, *LMA* leaf mass per area, V_{cmax} maximum velocity of Rubisco for carboxylation, J_{max} maximum rate of electron transport, *IPIF* Institute for Pacific Islands Forestry in Hilo, Hawaii

[a] Chemical and physiological values are given as the mean ± standard deviation (SD)

LMA ($r^2 = 0.28$), and the pigments ($r^2 < 0.1$) had weak correlations.

Canopy spectra

Canopy simulations using random LAI and LAD had much more spectral variation in the NIR (SD = 0.11 between 800 and 1,200 nm) than in canopy simulations with constant LAI and LAD (SD = 0.02 between 800 and 1,200 nm) (Fig. 5). When we used the full canopy spectral range (400–2,500 nm) for physiological predictions, there was initially no correlation. However, we then tested a variety of wavelengths, starting from 400–600 nm and going up to 400–2,500 nm in 50-nm increments. Predicting *A* with the minimum RMSE required a smaller spectral range at the canopy scale (400–900 nm, RMSE = 2.4 μmol m^{-2} s^{-1}) than at the leaf scale (400–2,400 nm, RMSE = 2.9 μmol m^{-2} s^{-1}) (Fig. 6). This was also evident for A_{max} and *R*, for which a canopy spectral range of 400–700 nm and 400–740 nm, respectively, was used to minimize RMSE. Canopy spectra were correlated with *A* ($r^2 = 0.61$, RMSE = 2.4 μmol m^{-2} s^{-1}), but only weakly correlated with A_{max} ($r^2 = 0.49$, RMSE = 4.7 μmol m^{-2} s^{-1}) and *R* ($r^2 = 0.16$, RMSE = 0.58 μmol m^{-2} s^{-1}) (Fig. 7). The canopy-scale weightings were largest near the red edge for *A* (Fig. 8). We only show canopy-scale weightings for *A* because both A_{max} and *R* have correlation coefficients of less than $r^2 = 0.5$. These regression models may not have sufficient precision to distinguish between different species because less than 50% of the variance in the data can be explained.

Discussion

Leaf-level photosynthesis predictions

Previous studies have shown that leaf spectra can be used to predict leaf chemical properties (Feret et al. 2008; Smith

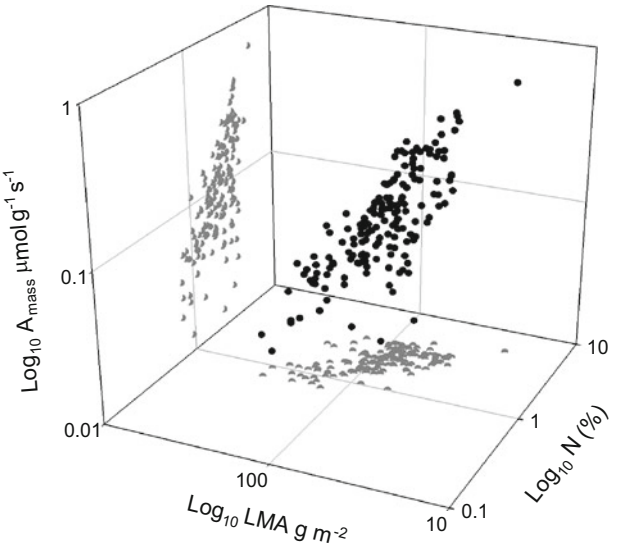

Fig. 2 Three-way scatterplot between mass-based leaf photosynthesis (A_{mass}, µmol g^{-1} s^{-1}), nitrogen (N, %), and leaf mass per area (LMA, g m^{-2}) using data collected from B2L and Hawaii. The axes are $\log_{10}$ transformed

et al. 2003a). Predictions of maximum photosynthetic capacity based on leaf spectra may be less accurate than those of leaf chemistry because leaf photosynthesis is not directly expressed in the spectra, but is instead a weighted combination of factors, including those of chemistry and LMA (Wright et al. 2004), both of which are directly expressed in the spectra (Jacquemoud and Baret 1990). We would expect a less accurate prediction of leaf physiological properties than chemical properties because the prediction error is a combination of the error in the spectral prediction of leaf chemical properties and the error inherent in the measurement of leaf physiological properties. In this study, predictions of photosynthesis based on leaf spectra are stronger than those of photosynthesis based solely on individual chemical properties, such as N or LMA, likely because leaf spectra integrate information on several chemical properties simultaneously. The RMSE of the predictions of light-saturated photosynthesis, but not R or A_{max}, were strong enough to predict differences between most tropical species (Fig. 3). We therefore have focused on light-saturated photosynthesis for most of this study.

Actual ambient photosynthesis of tropical ecosystems is often limited by stomatal closure, heat stress, and other environmental constraints (Doughty and Goulden 2008). Using spectra to predict A will not measure constraints on instantaneous photosynthesis, such as stomatal closure, which is not represented by the spectra. Instead, the spectra predict A in the absence of stomatal limitations. We minimized potentially confounding environmental stresses in our dataset by measuring photosynthetic capacity at optimum temperatures (25°C) and light levels (1,000 µmol m^{-2} s^{-1}). We also measured photosynthesis under CO_2 saturating concentrations (1,500 ppm) so that photosynthetic capacity would not change even if the stomata were partially closed. Despite our attempts to remove data where environmental stress was evident, we hypothesize that our physiology predictions of the B2L data had higher r^2 than those of the Hawaii data because the B2L data were collected in a controlled environment with minimal stress. Trees grown in the B2L may have fewer nutrient limitations than trees grown in Hawaii, which may be expressed in the relationship between leaf spectra and physiology.

We expected predictions of A_{max} to be stronger than those of A because measurements at very high CO_2 levels (1,500 ppm) will overcome any potential stomatal limitations and measure the maximum capacity regardless of conductance values. However, our regressions for A were stronger than those for $A_{max.}$ Light- and CO_2-saturated photosynthesis is limited because triose phosphate is released into the cytosol in exchange for an inorganic phosphate that is released during sucrose synthesis, and this rate of exchange sets an upper bound on CO_2-saturated photosynthesis (Sivak and Walker 1986). This mechanism is unlikely to be expressed by the spectra and may explain why CO_2-saturated photosynthesis had a weaker correlation than photosynthesis at ambient CO_2 concentrations.

The accuracy of many common land surface models used to predict canopy CO_2 fluxes depend on the proper representation of the kinetic properties of Rubisco, which are represented by V_{cmax} and J_{max}. J_{max} represents the light-limited state where photosynthesis is limited by electron transport, and V_{cmax} represents light-saturated conditions where photosynthesis is limited by the rate at which Rubisco can be regenerated. In our study, predictions of V_{cmax} and J_{max} were less accurate than those for the other physiological parameters. This is logical because the errors of the former are likely a summation of the error in the prediction of the chemical properties, the error in the physiological measurement, and the error in fitting a model to the physiology data to predict V_{cmax} and J_{max}.

Canopy photosynthesis predictions

Simulated canopy spectra with variable LAI and LAD show much variability in the NIR spectrum due to the effects of LAI on light scattering in the canopy (Myneni et al. 1989). This variability in the NIR spectrum increases the RMSE of our canopy photosynthesis predictions. Variable LAI and LAD will be present in the forests observed in most aircraft campaigns. However, the most important parts of the spectrum for predicting photosynthesis are in the visible and the red edge regions (Fig. 4). Therefore, our regressions show that the RMSE of the predictions of the photosynthesis at the canopy scale with unknown LAI

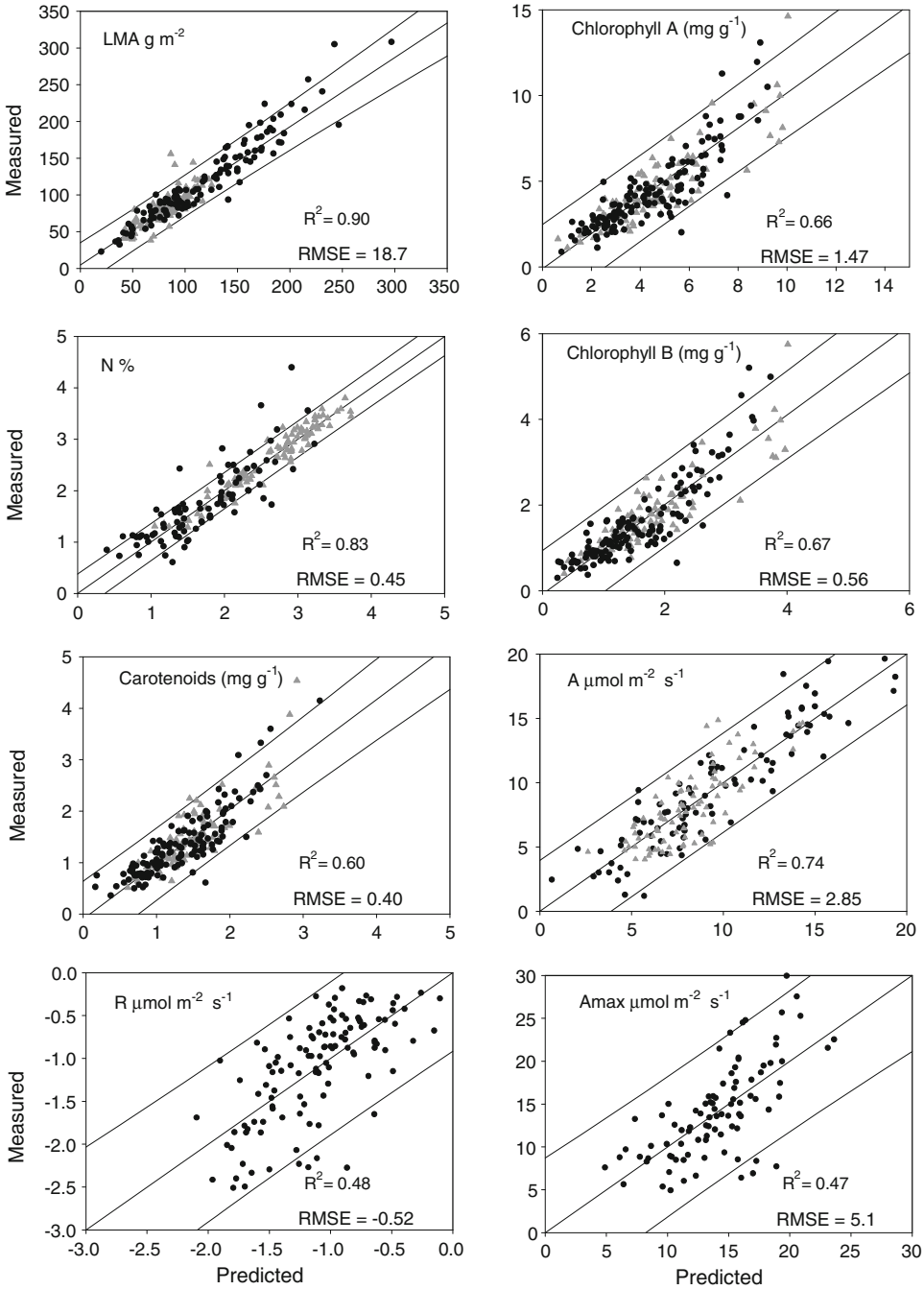

Fig. 3 Partial least squares (PLS) predictions of leaf chemical and physiological properties from leaf spectra from the Hawaii (*black dots*) and B2L (*dark grey triangles*) datasets (n = 159 species). *Outer lines* indicate 95% prediction intervals. *A* Light-saturated photosynthesis, A_{max} light- and CO_2-saturated photosynthesis, *R* respiration

and LAD is minimized using canopy spectra between 400 and 900 nm instead of the full spectral range (Fig. 6). This contrasts with predictions of photosynthesis using leaf-level spectrum, in which case RMSE was minimized using the full spectral range of 400–2,400 nm. The leaf-level spectrum does not have the multiple scattering in the NIR region that is present in canopy spectra and, therefore, there is a much smaller increase in spectral variability in the NIR. Without this increased spectral variability, the error is minimized at the leaf level by using the full spectral range.

The RMSE of photosynthesis predictions were slightly lower at the canopy level than at the leaf level (Fig. 6; RMSE = 2.5 ± 0.07 vs. 2.9 µmol m^{-2} s^{-1}, respectively), which corroborates chemical–spectral results from a previous study (Asner and Martin 2008). Canopy-level improvements are predicted by the radiative transfer theory which says that multiple scattering in the upper canopy leaf layers enhances the expression of leaf properties in highly foliated canopies (Baret et al. 1994).

A previous study found that large variations in LAI diminished canopy-level predictions of N, P, and leaf water

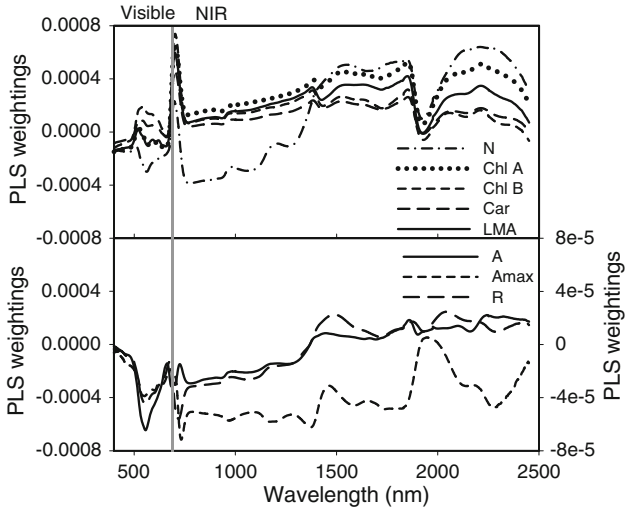

Fig. 4 PLS weightings using leaf transmittance spectra to predict leaf chemical properties (*top graph*), and physiological properties (*bottom graph*) from Hawaii and B2L. A *more positive or negative number* indicates a region of the spectrum that more strongly influences the regression model. The *grey vertical line* represents the boundary between the visible and the near-infrared (*NIR*) spectrum. *Chl* Chlorophyll, *Car* carotenoid

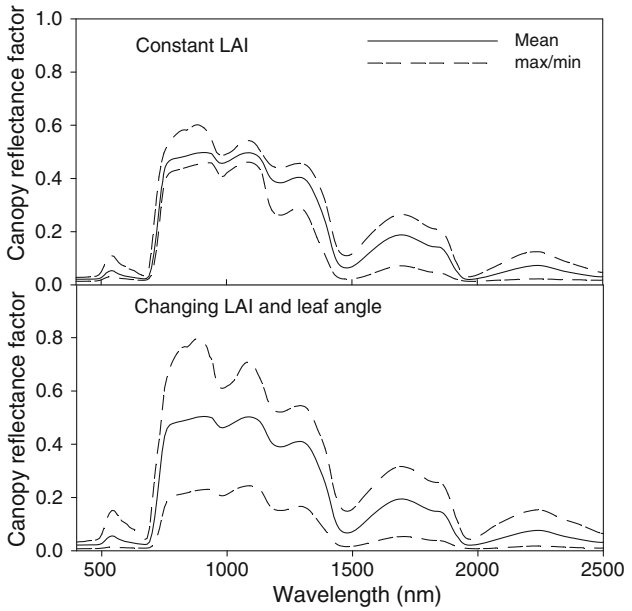

Fig. 5 Average canopy reflectance with constant leaf area index (*LAI*, 5) and leaf angle distribution (*top*), and with LAI ranging from 3–7 and variable leaf angle distribution (*bottom*)

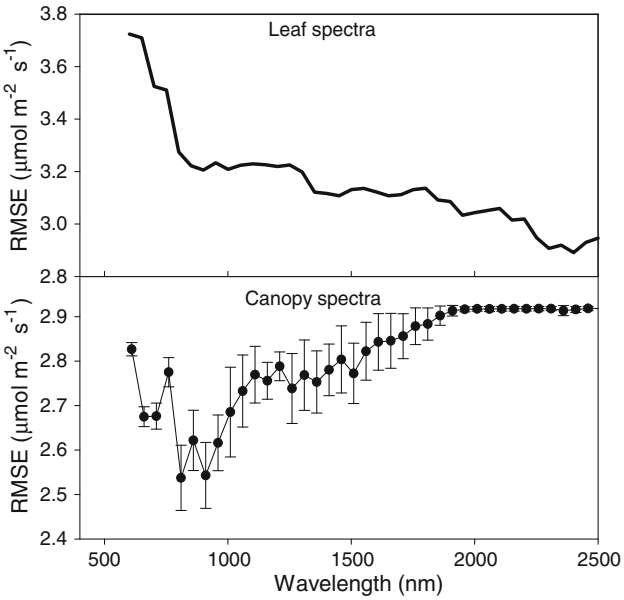

Fig. 6 Predictions of root means square error (*RMSE*) for leaf-level assimilation (*A*) using different spectral features for leaf transmittance (*top*) and canopy reflectance (*bottom*). Canopy spectra are the average ± SD of ten simulations with varied LAI and leaf angle distributions. The *x-axis* indicates the cumulative spectral range. For instance, a *point* at 1,000 nm on the *x-axis* indicates the RMSE for the prediction of photosynthesis using spectra ranging from 400 to 1,000 nm. All predictions use spectra starting at 400 nm

but did not diminish predictions of LMA or pigments (Asner and Martin 2008). The chemicals that are correlated with photosynthesis, such as N, are strongly expressed in the near-infrared portion of the reflectance spectrum (Kokaly 2001; Smith et al. 2003a), which is highly scattered in canopies. However, if wavelengths above 900 nm are removed, the visible and red edge signals remain, but noise in the NIR associated with multiple scatting from varied LAI is suppressed, resulting in a stronger prediction.

This technique represents an improvement on previous methods designed to remotely detect leaf-level physiology in tropical forests. The PLS methodology incorporates more spectral information than previous methods using individual spectral bands. This spectral information can accurately predict leaf N concentrations and LMA (Fig. 3), whose combination can explain much of the variability in leaf-level photosynthetic capacity (Wright et al. 2004). This method has a low enough RMSE (2.4 μmol m^{-2} s^{-1}) to predict differences in photosynthetic capacity between many individual upper canopy tropical tree species, which averaged 10.7 ± 4.3 μmol m^{-2} s^{-1} in one Amazonian study (Domingues et al. 2007).

We were able to measure photosynthetic capacity with both the Hawaii and B2L dataset. The spectral and chemical properties of these datasets were significantly different, which indicates that this technique may be valid under a range of conditions. Currently, this method cannot accurately detect other physiological properties, such as R, A_{max}, V_{cmax}, and J_{max}, and as it was tested primarily on species grown in Hawaiian botanical gardens with atypical forest structures, its broader applicability may be limited. Further tests are required to determine whether these data will be applicable to a broad range of tropical forests or just those

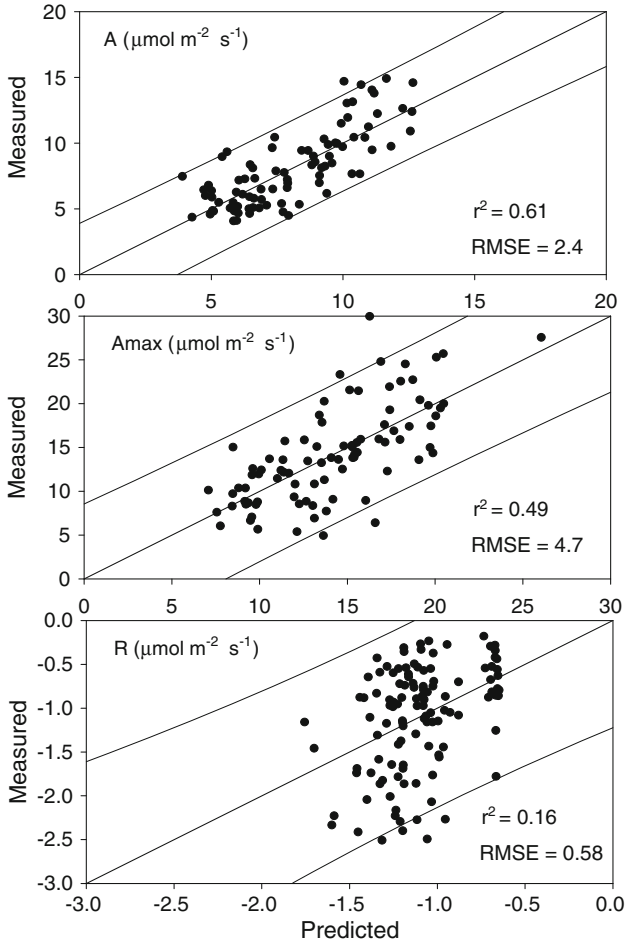

Fig. 7 Predictions of *A* (*top*, using spectra 400–900 nm, $n = 86$), A_{max} (*middle*, using spectra 400–700 nm, $n = 90$), and *R* (*bottom*, using spectra 400–740 nm, $n = 117$) from PLS regressions based on canopy spectra. Leaf spectra were scaled to canopy-level spectra using a radiative transfer model with variable LAI and leaf angle. *Outer lines* are 95% prediction intervals

in Hawaii and the B2L. We envision that this method will be useful for estimating tropical forest photosynthetic capacity in conjunction with methods that detect tropical forest carbon content.

Conclusions

We show that using the PLS regression technique on canopy spectra could lead to a better understanding of tropical forest leaf photosynthesis, with the potential of overcoming the traditional pitfalls of difficult canopy access and great tropical species diversity. We were able to predict light-saturated photosynthesis based on leaf transmittance and simulated canopy reflectance spectra with a sufficient level of accuracy (RMSE = 2.4 μmol m^{-2} s^{-1}) to detect photosynthetic differences between most species. An accurate understanding of photosynthetic capacity over a broad geographic area could lead to a better understanding of what drives carbon fluxes in tropical forests.

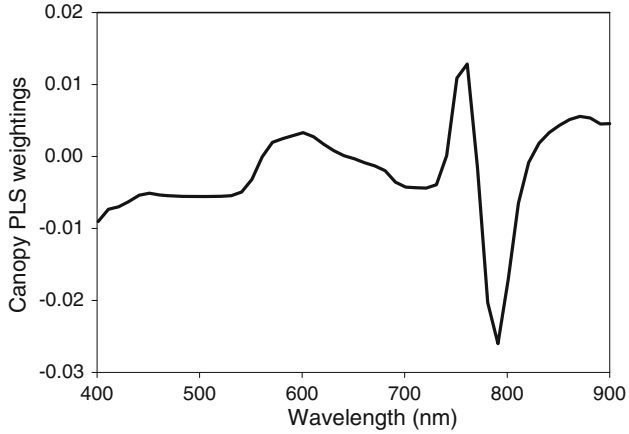

Fig. 8 PLS weightings for *A* ($n = 86$). We used only the wavelengths that minimize RMSE for *A* (400–900 nm). A more strongly positive or negative number indicates a part of the spectrum that more strongly influences the empirical model

Acknowledgments We thank K. Kinney, J. Kellner, and E. Broadbent for help in the field, and C. Field for advice. This work is funded by a Carnegie Institution fellowship, the NASA Terrestrial Ecology Biodiversity Program, and the John D. and Catherine T. MacArthur Foundation.

References

Asner GP, Martin RE (2008) Spectral and chemical analysis of tropical forests: scaling from leaf to canopy levels. Remote Sens Environ 112:3958–3970

Asner GP, Nepstad D, Cardinot G, Ray D (2004) Drought stress and carbon uptake in an Amazon forest measured with spaceborne imaging spectroscopy. Proc Natl Acad Sci USA 101: 6039–6044

Asner GP, Martin RE, Ford AJ, Metcalfe DJ, Liddell MJ (2009) Leaf chemical and spectral diversity in Australian tropical forests. Ecol Appl 19:236–253

Baret F, Vanderbilt VC, Steven MD, Jacquemoud S (1994) Use of spectral analogy to evaluate canopy reflectance sensitivity to leaf optical-properties. Remote Sens Environ 48:253–260

Castro-Esau KL, Sanchez-Azofeifa GA, Rivard B, Wright SJ, Quesada M (2006) Variability in leaf optical properties of Mesoamerican trees and the potential for species classification. Am J Bot 93:517–530

Curran P (1989) Global change and remote-sensing. Int J Remote Sens 10:1459–1460

Dempster WF (1999) Biosphere 2 engineering design. Ecol Eng 13:31–42

Domingues TF, Martinelli LA, Ehleringer JR (2007) Ecophysiological traits of plant functional groups in forest and pasture ecosystems from eastern Amazonia, Brazil. Plant Ecol 193:101–112

Doughty CE, Goulden ML (2008) Are tropical forests near a high temperature threshold? J Geophys Res-Biogeosciences 113. doi: 10.1029/2007JG000632

Farquhar GD, Caemmerer SV, Berry JA (1980) A biochemical-model of photosynthetic Co2 assimilation in leaves of C-3 species. Planta 149:78–90

Feret JB et al (2008) PROSPECT-4 and 5: advances in the leaf optical properties model separating photosynthetic pigments. Remote Sens Environ 112:3030–3043

Field CB, Behrenfeld MJ, Randerson JT, Falkowski P (1998) Primary production of the biosphere: integrating terrestrial and oceanic components. Science 281:237–240

Gitelson AA, Merzlyak MN (1997) Remote estimation of chlorophyll content in higher plant leaves. Int J Remote Sens 18:2691–2697

Grace J, Lloyd J, McIntyre J, Miranda AC et al (1995) Carbon-dioxide uptake by an undisturbed tropical rain-forest in Southwest Amazonia, 1992 to 1993. Science 270:778–780

Green RO, Eastwood ML, Sarture CM et al (1998) Imaging spectroscopy and the airborne visible infrared imaging spectrometer (AVIRIS). Remote Sens Environ 65:227–248

Haaland DM, Thomas EV (1988) Partial least-squares methods for spectral analyses 1 relation to other quantitative calibration methods and the extraction of qualitative information. Anal Chem 60:1193–1202

Jacquemoud S, Baret F (1990) PROSPECT—a model of leaf optical-properties spectra. Remote Sens Environ 34:75–91

Kokaly RF (2001) Investigating a physical basis for spectroscopic estimates of leaf nitrogen concentration. Remote Sens Environ 75:153–161

Lee DW, Bone RA, Tarsis SL, Storch D (1990) Correlates of leaf optical-properties in tropical forest sun and extreme-shade plants. Am J Bot 77:370–380

Lichtenthaler HK, Buschmann C (2001) Chlorophylls and carotenoids: measurement and characterization by UVVIS spectroscopy. Current Protocols in Food Analytical Chemistry

McGroddy ME, Daufresne T, Hedin LO (2004) Scaling of C:N:P stoichiometry in forests worldwide: implications of terrestrial redfield-type ratios. Ecology 85:2390–2401

Myneni RB, Ross J, Asrar G (1989) A review on the theory of photon transport in leaf canopies. Agric For Meteorol 45:1–153

Phillips OL, Malhi Y, Higuchi N, Laurance WF et al (1998) Changes in the carbon balance of tropical forests: evidence from long-term plots. Science 282:439–442

Poorter L, Bongers F (2006) Leaf traits are good predictors of plant performance across 53 rain forest species. Ecology 87:1733–1743

Saleska SR, Miller SD, Matross DM, Goulden M et al (2003) Carbon in amazon forests: unexpected seasonal fluxes and disturbance-induced losses. Science 302:1554–1557

Sellers PJ (1985) Canopy reflectance, photosynthesis and transpiration. Int J Remote Sens 6:1335–1372

Sharkey TD, Bernacchi CJ, Farquhar GD, Singsaas EL (2007) Fitting photosynthetic carbon dioxide response curves for C-3 leaves. Plant Cell Environ 30:1035–1040

Sims DA, Gamon JA (2002) Relationships between leaf pigment content and spectral reflectance across a wide range of species, leaf structures and developmental stages. Remote Sens Environ 81:337–354

Sivak MN, Walker DA (1986) Photosynthesis invivo can be limited by phosphate supply. New Phytol 102:499–512

Smith ML, Martin ME, Plourde L, Ollinger SV (2003a) Analysis of hyperspectral data for estimation of temperate forest canopy nitrogen concentration: comparison between an airborne (AVIRIS) and a spaceborne (Hyperion) sensor. IEEE Trans Geosci Remote Sens 41:1332–1337

Smith WK, Kelly RD, Welker JM, Fahnestock JT, Reiners WA, Hunt ER (2003b) Leaf-to-aircraft measurements of net CO_2 exchange in a sagebrush steppe ecosystem. J Geophys Res-Atmospheres 108(D3):15.1–15.9

Townsend AR, Cleveland CC, Asner GP, Bustamante MMC (2007) Controls over foliar N:P ratios in tropical rain forests. Ecology 88:107–118

Verma PK (1993) Remote-Sensing. Curr Sci 64:146–147

Wright IJ et al (2004) The worldwide leaf economics spectrum. Nature 428:821–827